J Neurophysiol 115: 3140–3145, 2016.
First published March 30, 2016; doi:10.1152/jn.00089.2016.

CALL FOR PAPERS | *Methods to Understand Brain Connections and Neural Function*

The functional organization of human epileptic hippocampus

Petr Klimes,[1,2,3] Juliano J. Duque,[1,4] Ben Brinkmann,[1,6] Jamie Van Gompel,[1,5] Matt Stead,[1,6] Erik K. St. Louis,[1,7] Josef Halamek,[2,3] Pavel Jurak,[2,3]* and Gregory Worrell[1,6]*

[1]*Mayo Systems Electrophysiology Laboratory, Department of Neurology, Mayo Clinic, Rochester, Minnesota;* [2]*Institute of Scientific Instruments of the CAS, Brno, Czech Republic;* [3]*International Clinical Research Center, St. Anne's University Hospital, Brno, Czech Republic;* [4]*Department of Computing and Mathematics, FFCLRP, University of São Paulo, Ribeirão Preto SP, Brazil;* [5]*Department of Neurosurgery, Mayo Clinic, Rochester, Minnesota;* [6]*Department of Biomedical Engineering and Physiology, Mayo Clinic, Rochester, Minnesota; and* [7]*Mayo Center for Sleep Medicine, Departments of Neurology and Medicine, Mayo Clinic, Rochester, Minnesota*

Submitted 1 February 2016; accepted in final form 29 March 2016

Klimes P, Duque JJ, Brinkmann B, Van Gompel J, Stead M, St Louis EK, Halamek J, Jurak P, Worrell G. The functional organization of human epileptic hippocampus. *J Neurophysiol* 115: 3140–3145, 2016. First published March 30, 2016; doi:10.1152/jn.00089.2016.—The function and connectivity of human brain is disrupted in epilepsy. We previously reported that the region of epileptic brain generating focal seizures, i.e., the seizure onset zone (SOZ), is functionally isolated from surrounding brain regions in focal neocortical epilepsy. The modulatory effect of behavioral state on the spatial and spectral scales over which the reduced functional connectivity occurs, however, is unclear. Here we use simultaneous sleep staging from scalp EEG with intracranial EEG recordings from medial temporal lobe to investigate how behavioral state modulates the spatial and spectral scales of local field potential synchrony in focal epileptic hippocampus. The local field spectral power and linear correlation between adjacent electrodes provide measures of neuronal population synchrony at different spatial scales, ~1 and 10 mm, respectively. Our results show increased connectivity inside the SOZ and low connectivity between electrodes in SOZ and outside the SOZ. During slow-wave sleep, we observed decreased connectivity for ripple and fast ripple frequency bands within the SOZ at the 10 mm spatial scale, while the local synchrony remained high at the 1 mm spatial scale. Further study of these phenomena may prove useful for SOZ localization and help understand seizure generation, and the functional deficits seen in epileptic eloquent cortex.

intracranial EEG; epilepsy; seizure onset zone; behavioral state; connectivity

NEW & NOTEWORTHY

Functional connectivity is reduced between seizure onset zone and surrounding brain tissue in human medial temporal lobe epilepsy. The reduced functional connectivity between the seizure onset zone and surrounding brain tissue is accentuated during slow-wave sleep. The functional organization within the seizure onset zone during sleep is characterized by increased local (~1 mm) high-frequency activity and reduced high-frequency connectivity at ~10 mm spatial scale.

THE ACTIVITY AND MUTUAL INTERACTIONS between local and distant neuronal populations underlie brain function. This cooperative activity gives rise to the local field potentials (LFP) (Einevoll et al. 2013; Mitzdorf 1985), and can be investigated at a range of spatial scales by analyzing the LFP spectral power from a single intracranial electrode, and statistical dependencies between LFPs recorded from multiple electrodes. The synchrony in LFP signals also provides a measure of functional connectivity between different brain regions (Brazdil et al. 2013; Bullmore and Sporns 2009; Horwitz 2003; van den Heuvel et al. 2012).

Focal epilepsy is characterized by a region of pathological, focal, epileptic brain generating spontaneous, unprovoked seizures (Lüders et al. 2006). The seizure onset zone (SOZ) is defined as the focal region of brain generating seizures, and generally overlaps with a wider region of brain that generates abnormal interictal epileptiform activity—interictal spikes and pathological high-frequency oscillations (pHFO) (Matsumoto et al. 2013; Spencer 2002; Staba et al. 2011; Worrell et al. 2012). The SOZ during interictal recordings (nonseizure recordings) are also known to exhibit increased high-frequency (>100 Hz) spectral power (Brazdil et al. 2010). In addition, prior studies have demonstrated alterations in focal epilepsy during interictal recordings using mean phase coherence (Mormann et al. 2000; Schevon et al. 2007), increased magnitude squared coherence (Zaveri et al. 2009), and increased nonlinear correlation (Bettus et al. 2008) as measures of LFP synchrony. The synchrony changes associated with focal epilepsy have also been used to investigate the functional connectivity between the SOZ and surrounding areas (Burns et al. 2014; Warren et al. 2010).

Changes in the LFP within the SOZ are also observed with different behavioral states. Slow-wave sleep is often associated with increased pathological epileptic activity (Bagshaw et al. 2009; Gloor et al. 1958; Staba et al. 2004). The effect of behavioral state on LFP activity and synchrony within the SOZ and non-SOZ has received less attention, and is explored here using combined sleep staging with intracranial EEG recordings.

Synchrony and connectivity of distinct neuronal populations is possible to define at different levels of spatial scale (Kötter

* P. Jurak and G. Worrell contributed equally to this work.
Address for reprint requests and other correspondence: G. Worrell, Dept. of Neurology, Mayo Clinic, 200 First St. SW, Rochester MN, 55905 (e-mail: worrell.gregory@mayo.edu).

2007; Sporns 2010). Intracranial macroelectrodes are often used to record LFP in medial temporal lobe brain structures, e.g., hippocampus and amygdala, in an effort to localize the seizure generators in focal epilepsy. The LFP measured with a clinical depth electrode is primarily comprised of the superposition of electrical activity from the synaptic currents within a volume of neural tissue in the neighborhood of the electrode (Mitzdorf 1985). Thus, increased LFP amplitude and spectral power can be interpreted as a measure of synchronized activity of local neuronal synapses, spatiotemporally filtered by the recording electrode (Katzner et al. 2009).

Implanted electrode arrays (multiple contacts on depth electrodes, see Fig. 1) provide an opportunity to investigate LFP characteristics and connectivity inside and outside SOZ at different spatial scales. The LFP spectral power, measured from a single depth electrode contact, provides a measure of local synchrony at a spatial scale of ~1 mm (a single depth electrode contact, Fig. 1). The LFP synchrony between two neighboring contacts (two neighboring contacts on a depth electrode separated by 10 mm, Fig. 1) provides a measure of more widespread, ~10 mm, synchrony. While there are multiple measures, a common measure of synchrony between two measured LFP signals is linear cross-correlation (Arunkumar et al. 2012; Schindler et al. 2007; Wang et al. 2014).

Both spectral power and linear correlation suffer from the common reference electrode contribution (Hu et al. 2010). There are multiple ways of suppressing the common component in measured signals (Schiff 2005; Zaveri et al. 2000), but none completely eliminate the reference contribution, and the data have to be interpreted with this knowledge. For example, in case of bipolar montage the signal is a measure of the difference in neuronal activity between the two regions recorded.

Our results provide an opportunity to investigate the highly local synchrony patterns inside and outside the pathological region of focal epileptic brain during different behavioral stages. Knowledge of local and wider spread synchrony behavior may ultimately prove useful for SOZ localization, understanding seizure generation and propagation, and the functional deficits associated with epilepsy.

METHODS

The Mayo Clinic Institutional Review Board approved the study, and all patients provided written informed consent. The patients underwent intracranial depth electrode implantation as part of their evaluation for epilepsy surgery when noninvasive studies could not adequately localize the SOZ (Fig. 1).

Table 1. *Patient data*

Patient	Age, yr	Sex	Number of Implanted (Processed) Electrodes	Duration of Sleep Recording, min	Duration of Wake Recording, min
1	34	F	16	30	10
2	28	F	16	20	20
3	21	F	12 (11)	30	30
4	39	M	8	30	30
5	33	F	16 (14)	10	20
6	47	M	16	20	20
7	22	F	16 (15)	30	30

Patients. Seven patients with medial temporal lobe focal epilepsy were investigated (see Table 1). All patients were implanted with intracranial depth electrodes; each depth electrode consists of either 4 or 8 contacts. The total number of processed channels from all 7 patients was 96. In addition, all patients had simultaneous scalp recordings for sleep scoring.

Electrodes and localization. Depth electrodes (AD-Tech Medical, Racine, WI) were 4 and 8 contact clinical depth electrodes consisting of a 1.3 mm diameter polyurethane shaft with Platinum/Iridium (Pt/Ir) clinical macroelectrode contacts; each contact is 2.3 mm long with 10 mm center-to-center spacing (surface area 9.4 mm^2 and impedance 200–500 ohms). Anatomical localization of electrodes was achieved using post-implant CT data coregistered to the patient's MRI space using normalized mutual information (SPM8, Fig. 1). Electrode coordinates were then automatically labeled by SPM Anatomy toolbox, with an estimated accuracy of 5 mm (Tzourio-Mazoyer et al. 2002).

Recordings. All intracranial EEG were acquired with a common reference, a stainless steel scalp suture placed in the vertex region of the scalp, midline between the international 10–20 Cz and Fz electrode positions. The scalp suture electrode was electrically insulated from the intracranial electrodes by the intervening layers of cerebrospinal fluid, bone, muscle and scalp. The data were acquired with a DC-capable Neuralynx electrophysiology system, digitized at 32 kHz. For analysis, the data were filtered using FIR bandpass filters from 0.5 to 1,000 Hz each with a Bartlett-Hanning window and decimated to a frequency of 5,000 Hz.

The SOZ localization. The SOZ electrodes and time of seizures were determined from the clinical report and verified independently by identifying the electrodes with the earliest intracranial EEG (iEEG) seizure discharge. Seizure onset times and location were determined by visual identification of a clear electrographic seizure discharge, followed by a look back in the iEEG recordings for the earliest electroencephalographic change contiguously associated with the sei-

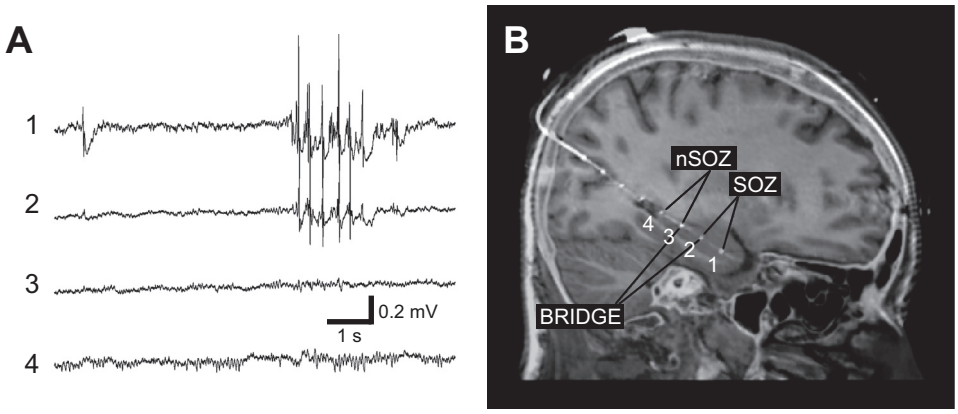

Fig. 1. Intracranial EEG and MRI-CT coregistered electrodes. *A*: the intracranial recording, i.e., local field potentials (LFP), from an 8 contact depth electrode implanted along the long axis of the hippocampus via a posterior approach. The anterior most *contact 1* targeting the anterior hippocampus and *contact 2* show interictal epileptiform spikes. In this patient *contacts 1–4* span the length of the hippocampus. *B*: the seizure onset zone (SOZ) was determined by recording spontaneous seizures and contacts outside the SOZ are denoted as non-SOZ (nSOZ). The contacts that bridge the SOZ and non-SOZ (here *3* and *2*) are labeled as bridge pairs.

zure. A similar approach was used for identification of neocortical SOZ (Warren et al. 2010; Worrell et al. 2004).

Sleep scoring. Visual sleep scoring was in accordance with standard methods (Iber et al. 2007) with modification for replacing the electrooculogram (EOG) recording with FP1, FP2, FPZ scalp electrodes. Wakefulness was determined by the presence of eye blinks visualized in FP1 and FP2, accompanied by posteriorly dominant alpha rhythms (8–12 Hz) comprising >50% of the epoch. N3 (slow-wave) sleep was scored when high-voltage (>75 μV) delta (0.5–2 Hz) frequency scalp EEG activity was present in at least 20% of the epoch (i.e., at least 6 s within a 30 s epoch) in the frontal derivations using conventional International 10–20 System (FP1, FP2, FZ, F3, F4, CZ, C3, C4, O1, O2, and Oz). A similar approach has been used in previous studies (Bower et al. 2015).

Data preprocessing. Prior to analysis, continuous scalp and intracranial EEG from each patient was reviewed using a custom MATLAB viewer (Brinkmann et al. 2009). Channels and time segments containing significant artifacts or seizures were not included in subsequent analysis. A specialized software tool SignalPlant (Plesinger et al. 2015) was used to identify interictal epileptiform spikes, followed by visual validation of detections. If an epileptiform spike was found on any channel, the data of all channels for that interval were omitted from analysis. In average, 1.3% of total length of signals was omitted; 1–3 awake and 1–3 sleep segments from interictal recordings, each 10 min long, were selected for each patient (160 min of wake and 170 min of sleep in total). To deal with the common-reference problem (Hu et al. 2010; Schiff 2005; Zaveri et al. 2000), the recordings were remontaged to unipolar signals referenced to the least active white matter intracranial electrode. Bipolar montage signals were created by subtracting the channel signal from its nearest neighboring electrode (difference of two adjacent contacts on the intracranial depth electrode). The data were filtered into eight frequency bands using bandpass Butterworth filters (delta 1–4 Hz, theta 4–8 Hz, alpha 8–12 Hz, beta 12–20 Hz, low gamma 20–55 Hz, high gamma 65–80 Hz, ripples 80–250 Hz and fast ripples 250–600 Hz). Unipolar signals referenced to white matter electrode were used for the LFP spectral power measurement. Bipolar signals were used for the bipolar spectral power measurement. In case of linear correlation calculation, unipolar signals referenced to the same relatively inactive white matter electrode were used due to a limited number of contacts in SOZ.

Spectral power. The spectral power levels of eight frequency bands in all channels were quantified by creating an average energy time series defined by $P(k) = E(k)/M$, where $k = 1,2,...$; $M = 500{,}000$ data points (100 seconds window); and $E(k) = \sum V^2(n)$, where $V(n)$ is the unipolar or bipolar voltage at discrete time n, and the sum runs from $n = 1 + (k - 1)M$ to $n = kM$. Average energy time series were calculated and used as a measure of average spectral power reflecting the synchrony at spatial scale of unipolar and bipolar derived potentials. In case of unipolar signals, the increased spectral power was interpreted as increased local synchrony at ~1 mm radius around single contact on intracranial electrode, while for bipolar recordings increased spectral power was interpreted as representing increased difference between the LFPs generated by neural assemblies separated by a spatial scale of ~10 mm, i.e., the distance between the adjacent electrodes.

Statistics: spectral power. For further analysis, the data were divided into two groups according to the channel location: inside SOZ (SOZ) and outside SOZ (non-SOZ). In case of bipolar power into three groups: SOZ (both neighboring contacts localized in SOZ), non-SOZ (both neighboring contacts localized outside SOZ) and BRIDGES (neighboring contacts inside and outside SOZ). To deal with different power levels in different patients (different recordings), power levels from each group were normalized to power in non-SOZ = 1. For statistical tests the different electrodes and pairs (SOZ, non-SOZ, BRIDGE) were aggregated together over patients. Statistical differences between groups were tested using the nonparametric Wilcoxon rank sum test. Results are shown for $P < 0.05$ and $P < 0.01$.

Linear correlation. For a measure of neuronal synchrony at spatial scale of ~10 mm, continuous linear correlations of lag $n = 0$ between nearest neighbor contacts on each depth electrode were calculated. For synchrony analysis, balancing the issues of signal nonstationarity and adequate sample size, we selected sliding window of size from 8 s to 500 ms (8 s for delta 1–4 Hz, 3 s for theta 4–8 Hz, 2 s for alpha 8–12 Hz, 1 s for beta 12–20 Hz and 500 ms for low gamma 20–55 Hz and all higher frequencies). Too narrow window can produce errors by correlating short samples of signals and wide window can average out important dynamics in the signals. The sliding analysis windows had a 10% overlap. For each step of sliding windows the Pearson's correlation coefficient was calculated between two neighboring channels on electrode. For further analysis, median values of correlation coefficients were taken from non-overlapped 100 s segments.

Statistics: correlation. Subsequently, correlation values were divided into three groups: SOZ (both channels in analyzed pair were localized in SOZ), non-SOZ (both channels outside of SOZ) and BRIDGES (one channel in and one channel out of SOZ region). For statistic tests the groups were aggregated together over patients. To determine statistical differences between groups the Kruskall-Wallis test and nonparametric Wilcoxon rank sum tests were used. Levels of significance were considered $P < 0.05$ and $P < 0.01$.

RESULTS

During slow-wave sleep, unipolar power (see Fig. 3*A*) was increased in SOZ compared with non-SOZ, suggesting that the local synchrony at spatial scale ~1 mm was increased in SOZ. Synchrony during sleep determined by linear correlation (Fig. 2*A*) was increased in SOZ compared with non-SOZ over frequency bands delta, theta, alpha, beta, and low gamma (1–55 Hz). Synchrony in SOZ in higher frequency bands dropped and in ripples and fast ripples crossed-over to the lowest value, supporting the hypothesis of fractured functional organization of the SOZ with islands generating independent, uncorrelated, increased high-frequency activity. The lowest synchrony was demonstrated between electrodes that bridge SOZ and non-SOZ, consistent with the reduced functional connectivity between the SOZ and the surrounding areas.

Similarly, during wakefulness the connectivity determined by correlation (Fig. 2*B*) between bridging electrodes was reduced compared with electrodes within the SOZ, which were again strongly synchronized. However, during wakefulness the SOZ connectivity cross-over to the lowest connectivity in ripples and fast ripples was not observed, although the synchrony level in SOZ is lower in fast ripples compared with lower frequencies. The unipolar power during wake state (Fig. 3*B*) was higher in SOZ. Differences of unipolar power between SOZ and non-SOZ were reduced during wake state compared with slow-wave sleep.

The bipolar spectral power levels show relative changes between SOZ, non-SOZ and bridges (Fig. 2, *C* and *D*). During slow-wave sleep, the bipolar power was increased in SOZ compared with non-SOZ for all frequency bands. The bipolar power in areas bridging SOZ and non-SOZ was increased compared with non-SOZ areas for all frequency bands except fast ripples, with a peak in high gamma band and consistent with uncorrelated activity in SOZ and non-SOZ (Fig. 2*A*).

During wake, the bipolar power (Fig. 2*D*) was the highest in SOZ in higher frequencies, especially in high gamma and ripple frequency band. SOZ and bridging areas were lower than non-SOZ in theta and alpha band. The differences be-

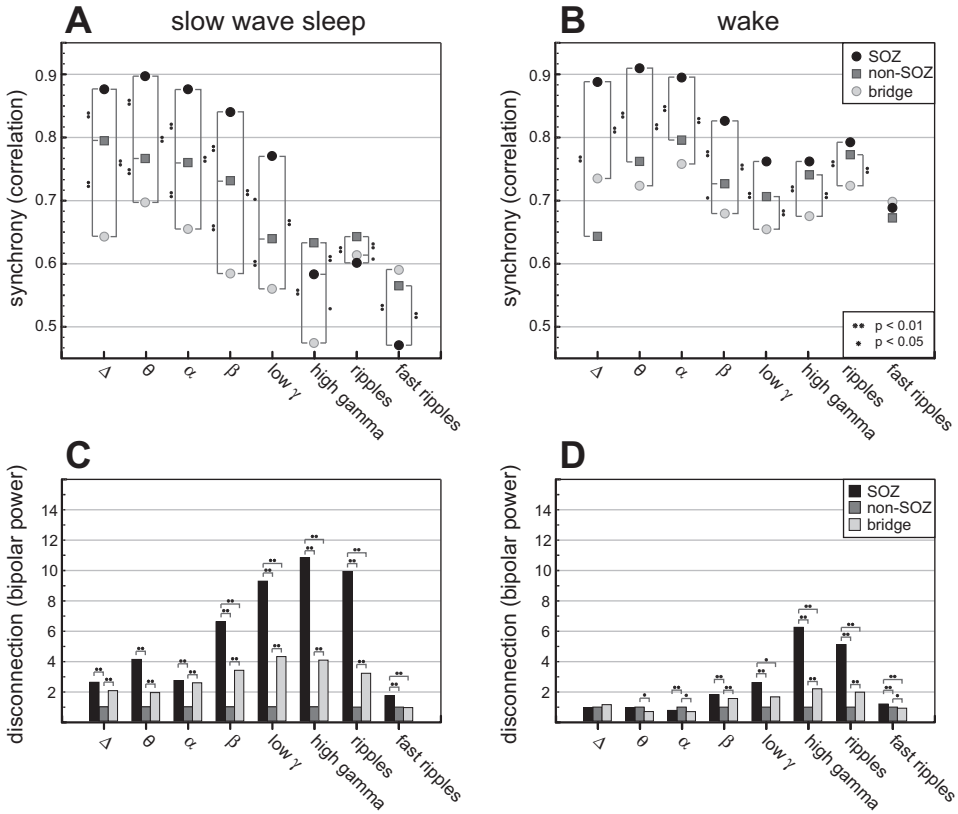

Fig. 2. Ten-millimeter spatial scale synchrony (correlation, bipolar power), and behavioral state modulation (top). The linear correlation between electrode pairs located in SOZ, non-SOZ, and bridging areas in the delta (1–4 Hz), theta (4–8 Hz), alpha (8–12 Hz), beta (12–20 Hz), low gamma (20–55 Hz), high gamma (65–80 Hz), ripples (80–250 Hz), and fast ripples (250–600 Hz) frequency bands. During sleep (left top, *A*), the correlation is increased in SOZ compared with non-SOZ at frequencies delta-beta, but exhibits a cross-over to low connectivity in higher frequency bands within the SOZ. The connectivity between electrodes that bridge SOZ and non-SOZ (bridging electrode pairs) exhibit lower connectivity compared with SOZ and non-SOZ, except at ripples and fast ripples. Similarly, during wakefulness (right top, *B*) the connectivity between bridging electrodes is reduced compared with electrodes within the SOZ and non-SOZ (*bottom*) The bipolar power is calculated from the difference of two adjacent electrode LFPs. Relative changes of bipolar power between groups − bipolar power values at each frequency are normalized to power outside SOZ = 1. During slow-wave sleep (left bottom, *C*) the bipolar power is increased in SOZ compared with non-SOZ for all frequency bands, supporting a relative statistical independence of the activity at adjacent electrodes in the SOZ compared with electrodes in the non-SOZ. The highest power is in high gamma. The bipolar power in areas bridging SOZ and non-SOZ is increased compared with non-SOZ areas for all frequency bands except fast ripples, supporting that the connectivity between SOZ and non-SOZ is reduced. During wake (right bottom, *D*) the bipolar power is the highest in SOZ in high gamma. The bipolar power in SOZ and bridging areas is lower than non-SOZ in theta and alpha band. The differences between bipolar power in SOZ-non-SOZ and bridges-non-SOZ are lower for all frequency bands compared with slow-wave sleep. Statistical difference between groups is observed at two levels, $*P < 0.05$ and $**P < 0.01$.

tween bipolar power in SOZ-non-SOZ and bridges-non-SOZ during wake were lower for all frequency bands compared with slow-wave sleep. Increased values of bipolar power in SOZ support increased LFPs differences at a spatial scale ~10 mm, within SOZ at higher frequencies. Increased bipolar power for bridge configurations provide evidence for reduced connectivity between SOZ region and surrounding areas (Fig. 2*B*).

DISCUSSION

We show that LFP spectral power is increased in the SOZ compared with surrounding brain (non-SOZ), and that the synchrony between electrodes bridging the SOZ and non-SOZ is reduced, consistent with reduced functional connectivity between SOZ and non-SOZ (Warren et al. 2010). The reduced

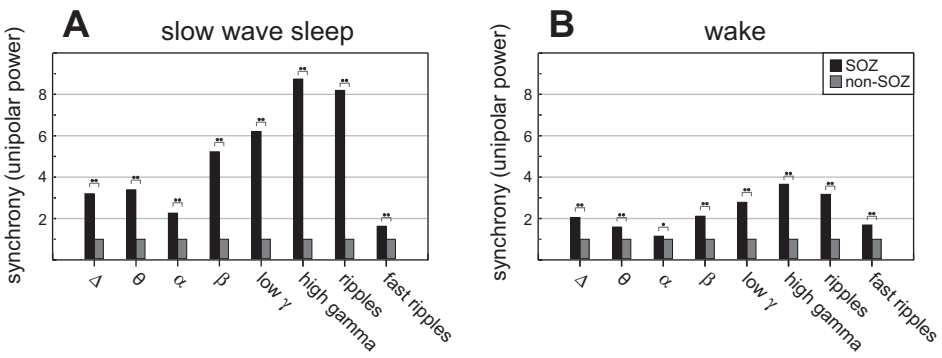

Fig. 3. One-millimeter spatial scale synchrony (unipolar power), and behavioral state modulation. The LFP unipolar spectral power from a single electrode can be interpreted as a local (~1 mm) measure of neuronal synchrony (power normalized to non-SOZ = 1). The LFP unipolar power is increased in SOZ compared with non-SOZ for all frequency bands, during both behavioral states [slow-wave sleep (*A*), wake (*B*)]. The difference between SOZ and non-SOZ is reduced during wakefulness in alpha band. In general, differences between SOZ and non-SOZ were smaller during wake state. Statistical difference between groups is observed at two levels, $*P < 0.05$ and $**P < 0.01$.

connection between SOZ and surrounding brain shown here in medial temporal lobe epilepsy occurs over a wide range of frequencies, and is accentuated during slow-wave sleep. This result is similar to our previous findings in neocortical SOZ during wakefulness (Warren et al. 2010). In addition, while the local synchrony probed by the LFP spectral power is increased in the SOZ at the spatial scale sampled by a single clinical depth electrode contact (~1 mm) over a wide range of frequency (1–600 Hz) the synchrony between adjacent electrode contacts (separated by 10 mm) drops precipitously at higher frequencies in the SOZ compared with non-SOZ (Fig. 2, *A* and *B*, gamma, ripple, fast ripple bands; Fig. 2*C*, beta, gamma, ripple, fast ripple bands; Fig. 2*D*, gamma, ripple, fast ripple bands). During sleep, at this longer spatial scale of ~10 mm the synchrony measure drop to values below pairs bridging SOZ and non-SOZ (Fig. 2*A*, ripple, fast ripples bands).

These results support a model of increased synchrony within the local assemblies generating high frequency activity (Kucewicz et al. 2014) in the SOZ at the spatial scale of ~1 mm, but the increased synchrony breaks down at larger spatial scales (~10 mm) for neuronal assemblies that generate LFP activity in the high frequency range (>65 Hz). This finding is consistent with the SOZ itself composed of islands separated by reduced functional connectivity (<10 mm), and with the hypothesis that the generators of high-frequency oscillations are more spatially localized (Bragin et al. 2000; Logothetis et al. 2007). This phenomenon is also consistent with our previous results using microelectrode arrays to record microdomain seizure activity (Stead et al. 2010). The synchrony behavior during wakefulness is similar to slow-wave sleep, but the local synchrony is reduced in the SOZ compared with non-SOZ. This suggests that the LFP activity associated with normal function is disrupted in the SOZ.

The linear correlation indicates a loss of the statistical interdependency of LFP measured at the different recording sites. The decrease in statistical interdependency of LFP from two regions could be due to an actual loss of physical connections between these two regions, as might occur from loss of synaptic connections between neurons in these two regions, or related to the local neuronal assemblies generating the LFP at each site. The mechanism cannot be elucidated by our data, but possibilities include disruption of synaptic connections between neurons in the different regions or reorganization of synaptic connections within the SOZ. Epileptiform sharp wave occurring independently in SOZ but not in non-SOZ would result in very different filtered LFPs in each region and yield a low correlation. To address this possibility, however, we removed interictal epileptiform sharp waves from each data channel and recalculated the synchrony measures. We found that epileptiform activity does affect the result, but the decreased correlation between different brain regions remains significant after removal of epileptiform activity.

In summary, we show evidence for reduced connection between epileptic medial temporal lobe in human partial epilepsy and surrounding brain regions, and that the SOZ itself is composed of islands generating high frequency activity that is independent of surrounding SOZ assemblies. We can speculate that functional disconnection within the SOZ itself, and with surrounding non-SOZ tissue, may be a clinically useful electrophysiological signature of epileptic brain. Knowledge of these principles may prove useful for SOZ localization, understanding seizure generation, propagation, and the functional deficits seen in eloquent cortex when disrupted by focal epilepsy.

ACKNOWLEDGMENTS

We acknowledge Cindy Nelson and Karla Crockett for technical support, and Amit Chopra, M.D. and Paul Shepard for assistance with sleep scoring.

GRANTS

This research was supported by Mayo Clinic Discovery Translation Grant, National Institutes of Health (R01-NS063039, R01-NS078136, and UH2-NS095495), Grant agency of the Czech Republic (P103/11/0933), European Regional Development Fund-Project FNUSA-ICRC (CZ.1.05/1.1.00/02.0123), MEYS CR and EC (CZ.1.05/2.1.00/01.0017), ALISI-NPU (LO1212), VES15 II-LH15047, and São Paulo Research Foundation 2014/01587-8.

DISCLOSURES

No conflicts of interest, financial or otherwise, are declared by the author(s).

AUTHOR CONTRIBUTIONS

P.K., J.J.D., P.J., and G.W. conception and design of research; P.K., J.J.D., and E.K.S.L. analyzed data; P.K., J.J.D., J.H., P.J., and G.W. interpreted results of experiments; P.K., J.J.D., and B.B. prepared figures; P.K. drafted manuscript; P.K., J.J.D., B.B., J.H., P.J., and G.W. edited and revised manuscript; P.K., J.J.D., B.B., J.V.G., M.S., E.K.S.L., J.H., P.J., and G.W. approved final version of manuscript; J.V.G. and M.S. performed experiments.

REFERENCES

Arunkumar A, Panday A, Joshi B, Ravindran A, Zaveri HP. Estimating correlation for a real-time measure of connectivity. *Conf Proc IEEE Eng Med Biol Soc* 2012: 5190–5193, 2012. doi:10.1109/EMBC.2012.6347163.

Bagshaw AP, Jacobs J, LeVan P, Dubeau F, Gotman J. Effect of sleep stage on interictal high-frequency oscillations recorded from depth macroelectrodes in patients with focal epilepsy. *Epilepsia* 50: 617–628, 2009. doi:10.1111/j.1528–1167.2008.01784.x.

Bettus G, Wendling F, Guye M, Valton L, Régis J, Chauvel P, Bartolomei F. Enhanced EEG functional connectivity in mesial temporal lobe epilepsy. *Epilepsy Res* 81: 58–68, 2008. doi:10.1016/j.eplepsyres.2008.04.020.

Bower MR, Stead M, Bower RS, Kucewicz MT, Sulc V, Cimbalnik J, Brinkmann BH, Vasoli VM, St Louis EK, Meyer FB, Marsh WR, Worrell GA. Evidence for consolidation of neuronal assemblies after seizures in humans. *J Neurosci* 35: 999–1010, 2015. doi:10.1523/JNEUROSCI.3019–14.2015.

Bragin A, Wilson CL, Engel J. Chronic epileptogenesis requires development of a network of pathologically interconnected neuron clusters: a hypothesis. *Epilepsia* 41: S144–S152, 2000.

Brazdil M, Halamek J, Jurak P, Daniel P, Kuba R, Chrastina J, Novák Z, Rektor I. Interictal high-frequency oscillations indicate seizure onset zone in patients with focal cortical dysplasia. *Epilepsy Res* 90: 28–32, 2010. doi:10.1016/j.eplepsyres.2010.03.003.

Brazdil M, Janecek J, Klimes P, Marecek M, Roman R, Jurak J, Chladek J, Daniel P, Rektor I, Halamek J, Plesinger F, Jirsa V. On the time course of synchronization patterns of neuronal discharges in the human brain during cognitive tasks. *PloS One* 8: e63293, 2013. doi:10.1371/journal.pone.0063293.

Brinkmann BH, Bower MR, Stengel KA, Worrell GA, Stead M. Large-scale electrophysiology: acquisition, compression, encryption, and storage of big data. *J Neurosci Methods* 180: 185–192, 2009.

Bullmore E, Sporns O. Complex brain networks: graph theoretical analysis of structural and functional systems. *Nat Rev Neurosci* 10: 186–198, 2009.

Burns SP, Santaniello S, Yaffe RB, Jouny CC, Crone NE. Network dynamics of the brain and influence of the epileptic seizure onset zone. *Proc Natl Acad Sci USA* 111: E5321–E5330, 2014. doi:10.1073/pnas.1401752111.

Einevoll GT, Kayser C, Logothetis NK, Panzeri S. Modelling and analysis of local field potentials for studying the function of cortical circuits. *Nat Rev Neurosci* 14: 770–785, 2013. doi:10.1038/nrn3599.

Gloor P, Tsai C, Haddad F. An assessment of the value of sleep-electroencephalography for the diagnosis of temporal lobe epilepsy. *Electroencephalogr Clin Neurophysiol* 10: 633–648, 1958.

Horwitz B. The elusive concept of brain connectivity. *Neuroimage* 19: 466–470, 2003.

Hu S, Stead M, Dai Q, Worrell GA. On the recording reference contribution to EEG correlation, phase synchrony, and coherence. *IEEE Trans Syst Man Cybern B Cybern* 40: 1294–1304, 2010. doi:10.1109/TSMCB.2009.2037237.

Iber C, Ancoli-Israel S, Chesson A, Quan SF; the American Academy of Sleep Medicine. *The AASM Manual for the Scoring of Sleep and Associated Events: Rules, Terminology and Technical Specifications*. Westchester, IL: American Academy of Sleep Medicine, 2007.

Katzner S, Nauhaus I, Benucci A, Bonin V, Ringach DL, Carandini M. Local origin of field potentials in visual cortex. *Neuron* 61: 35–41, 2009. doi:10.1016/j.neuron.2008.11.016.

Kötter R. Anatomical concepts of brain connectivity. In: *Handbook of Brain Connectivity*, Series: Understanding Complex Systems, edited by Jirsa V, McIntosh AR. Berlin: Springer, 2007, p. 149–166.

Kucewicz MT, Cimbalnik J, Matsumoto JY, Brinkmann BH, Bower MR, Vasoli V, Sulc V, Meyer F, Marsh WR, Stead SM, Worrell GA. High frequency oscillations are associated with cognitive processing in human recognition memory. *Brain* 137: 2231–2244, 2014. doi:10.1093/brain/awu149.

Logothetis NK, Kayser C, Oeltermann A. In vivo measurement of cortical impedance spectrum in monkeys: Implications for signal propagation. *Neuron* 55: 809–823, 2007.

Lüders HO, Najm I, Nair D, Widdess-Walsh P, Bingman W. The epileptogenic zone: general principles. *Epileptic Disord* 8, *Suppl* 2: S1–S9, 2006.

Matsumoto JY, Stead M, Kucewicz MT, Matsumoto AJ, Peters PA, Brinkmann BH, Danstrom JC, Goerss SJ, Marsh WR, Meyer FB, Worrell GA. Network oscillations modulate interictal epileptiform spike rate during human memory. *Brain* 136: 2444–2456, 2013. doi:10.1093/brain/awt159.

Mitzdorf U. Current source-density method and application in cat cerebral cortex: investigation of evoked potentials and EEG phenomena. *Physiol Rev* 65: 37–100, 1985.

Mormann F, Lehnertz K, David P, Elger EC. Mean phase coherence as a measure for phase synchronization and its application to the EEG of epilepsy patients. *Physica D Nonlinear Phenomena* 144: 358–369, 2000.

Plesinger F, Jurco J, Halamek J, Jurak P. *SignalPlant*. Brno, Czech Republic: Institute of Scientific Instruments of CAS. Retrieved from https://signalplant.codeplex.com.

Schevon CA, Cappell J, Emerson R, Isler J, Grieve P, Goodman R, McKhann G, Weiner H, Doyle W, Kuzniecky R, Devinsky O, Gilliam F. Cortical abnormalities in epilepsy revealed by local EEG synchrony. *Neuroimage* 35: 140–148, 2007.

Schiff SJ. Dangerous phase. *Neuroinformatics* 3: 315–318, 2005.

Schindler K, Elger CE, Lehnertz K. Increasing synchronization may promote seizure termination: evidence from status epilepticus. *Clin Neurophysiol* 118: 1955–1968, 2007.

Spencer SS. Neural networks in human epilepsy: evidence of and implications for treatment. *Epilepsia* 43: 219–227, 2002.

Sporns O. *Networks of the Brain*. MIT Press, 2010.

Staba RJ, Wilson CL, Bragin A, Jhung D, Fried I, Engel J. High-frequency oscillations recorded in human medial temporal lobe during sleep. *Annals Neurol* 56: 108–115, 2004.

Staba RJ, Bragin A. High-frequency oscillations and other electrophysiological biomarkers of epilepsy: Underlying mechanisms. *Biomark Med* 5: 545–556, 2011.

Stead M, Bower M, Brinkmann BH, Lee K, Marsh WR, Meyer FB, Litt B, Gompel JV, Worrell GA. Microseizures and the spatiotemporal scales of human partial epilepsy. *Brain* 133: 2789–2797, 2010.

Tzourio-Mazoyer N, Landeau B, Papathanassiou D, Crivello F, Etard O, Delcroix N, Mazoyer B, Joliot M. Automated anatomical labeling of activations in SPM using a macroscopic anatomical parcellation of the MNI MRI single-subject brain. *Neuroimage* 15: 273–289, 2002.

van den Heuvel MP, Kahn RS, Goñi J, Sporns O. High-cost, high-capacity backbone for global brain communication. *Proc Natl Acad Sci USA* 109: 11372–11377, 2012. doi:10.1073/pnas.1203593109.

Wang HE, Bénar CG, Quilichini PP, Friston KJ, Jirsa VK, Bernard C. A systematic framework for functional connectivity measures. *Front Neurosci* 8: 1–22, 2014. doi:10.3389/fnins.2014.00405.

Warren CP, Hu S, Stead M, Brinkmann BH, Bower MR, Worrell GA. Synchrony in normal and focal epileptic brain: the seizure onset zone is functionally disconnected. *J Neurophysiol* 104: 3530–3539, 2010.

Worrell GA, Parish L, Cranstoun SD, Jonas R, Baltuch G, Litt B. High-frequency oscillations and seizure generation in neocortical epilepsy. *Brain* 127: 1496–1506, 2004.

Worrell GA, Jerbi K, Kobayashi K, Lina JM, Zelmann R, Le Van Quyen M. Recording and analysis techniques for high-frequency oscillations. *Prog Neurobiol* 98: 265–278, 2012.

Zaveri HP, Duckrow RB, Spencer SS. The effect of a scalp reference signal on coherence measurements of intracranial electroencephalograms. *Clin Neurophysiol* 111: 1293–1299, 2000.

Zaveri HP, Pincus SM, Goncharova II, Duckrow RB, Spencer DD, Spencer SS. Localization-related epilepsy exhibits significant connectivity away from the seizure onset area. *Neuroreport* 20: 891–895, 2009.